

Rafał BRYK
Holger SCHMIDT
Thomas MULL

MODELING OF EMERGENCY CONDENSER SYSTEM RESPONSE TO LOSS OF COOLANT ACCIDENT IN A BWR III+ GENERATION

MODELOWANIE ZACHOWANIA SYSTEMU KONDENSATORA AWARYJNEGO W PRZYPADKU AWARII UTRATY CHŁODZIWA W REAKTORZE BWR GENERACJI III+

Emergency Condenser (EC) is a heat exchanger composed of a large number of slightly inclined U-tubes arranged horizontally. The inlet header of the condenser is connected with the top part of the Reactor Pressure Vessel (RPV), which is occupied by steam during critical operation. The lower header in turn is linked with the RPV below the liquid water level during normal operation of the reactor. The tube bundle is filled with cold water and it is located in a vessel filled with water of the same temperature. Thus, the EC and RPV form together a system of communicating vessels. In case of an emergency and a decrease of the water level in the RPV, the water flows gravitationally from U-tubes to the RPV. At the same time the steam from the RPV enters to the EC and condenses due to its contact with cold walls of the EC. The condensate flows then back to the RPV due to the tubes inclination. Hence, the system removes heat from the RPV and serves as a high- and low-pressure injection system at the same time. In this paper a model of the EC system is presented. The model was developed with Modelica modeling language and OpenModelica environment which had not been used in this scope before. The model was verified against experimental data obtained during tests performed at INKA (Integral Test Facility Karlstein) – a test facility dedicated for investigation of the passive safety systems performance of KERENA – generation III+ BWR developed by Framatome.

Keywords: boiling water reactor, emergency condenser, LOCA, Modelica.

Kondensator awaryjny jest wymiennikiem ciepła złożonym z dużej ilości U-rurek lekko nachylonych względem pozycji horyzontalnej. Kolektor wlotowy kondensatora połączony jest pojedynczym przewodem z górną częścią zbiornika ciśnieniowego reaktora, w której w trakcie normalnej pracy reaktora znajduje się para wodna. Dolny kolektor połączony jest natomiast ze zbiornikiem ciśnieniowym poniżej lustra wody w stanie ciekłym. Wiązka rurek kondensatora, w trakcie krytycznej pracy reaktora, wypełniona jest zimną wodą i zanurzona jest w basenie z wodą o tej samej temperaturze. Wiązka rurek kondensatora oraz rur doprowadzających tworzą wraz ze zbiornikiem ciśnieniowym zespół naczyń połączonych. W razie sytuacji awaryjnej, w przypadku spadku poziomu wody w zbiorniku ciśnieniowym, woda z kondensatora spływa grawitacyjnie do zbiornika ciśnieniowego, a para, która dostaje się do U-rurek kondensuje na skutek wymiany ciepła z zimną wodą otaczającą kondensator od zewnątrz. W ten sposób kondensator działając pasywnie, zastępuje wysokociśnieniowy oraz niskociśnieniowy wtrysk wody chłodzącej do zbiornika ciśnieniowego. W artykule przedstawiono model systemu kondensatora awaryjnego wraz ze zbiornikiem ciśnieniowym. Model został wykonany przy użyciu niestosowanego wcześniej w tym zakresie języka Modelica oraz środowiska OpenModelica. Następnie opracowany kod został zweryfikowany poprzez porównanie wyników z pomiarami eksperymentalnymi przeprowadzonymi na obiekcie INKA (Integral Test Facility Karlstein) – obiekcie testowym dedykowanym badaniom nad pasywnymi systemami bezpieczeństwa reaktora KERENA – reaktora BWR generacji III+ opracowanego przez firmę Framatome.

Słowa kluczowe: reaktor wodny wrzący, kondensator awaryjny, awaria utraty chłodziwa, Modelica.

Nomenclature

Latin symbols		Greek symbols	
A	Cross section [m ²]	α	Heat transfer coefficient [W/m ² /K]
BWR	Boiling Water Reactor	β	Expansion coefficient [1/K]
c	Specific Heat capacity [J/(kgK)]	κ	Thermal diffusivity [m ² /s]
D	Diameter [m]	λ	Thermal conductivity [W/(mK)]
E	Energy [J]	μ	Dynamic viscosity [Pa s]
EC	Emergency Condenser	ν	Kinematic viscosity [m ² /s]
FPV	Flooding Pool Vessel	ρ	Density [kg/m ³]
g	Gravity acceleration [m/s ²]		

h	Specific enthalpy [J/kg]	Subscripts	
L	Length of the whole tube [m]	cs	Condensation
l	Length of a single volume [m]	evap	Evaporation
M	Mass [kg]	f	Friction
\dot{m}	Mass flow rate [kg/s]	g	Gravity
Nu	Nusselt number	infl	Tube inlet
p	Pressure [Pa]	l	Liquid
Pr	Prandtl number	ls	Liquid saturation
Ra	Rayleigh number	outfl	Tube outlet
Re	Reynolds number	p	At constant pressure
RPV	Reactor Pressure Vessel	sat	Saturation
\dot{Q}	Heat flow rate [W]	SP	Single-phase
\dot{q}	Heat flux [W/m ²]	v	Vapor
T	Temperature [K]	vs	Vapor saturation
u	Flow velocity [m/s]	w	Wall
V	Volume [m ³]		
x	Steam quality		
z	Water level [m]		

1. Introduction

During the last decades, a lot of efforts have been undertaken to increase the safety of nuclear reactors. These efforts were mainly targeted to develop the concept of passive safety, in which the human factor is eliminated. The modern nuclear reactor designs do not require any external power supply like a Diesel engine or an electrical motor to provide proper cooling to the nuclear reactor core in case of loss of coolant. They function according to fundamental laws of physics such as gravity and free convection.

A common approach to measure safety of a technical facility is Quantitative Risk Analysis or Probabilistic Safety Assessment. These terms are used synonymously in different industries. In the analysis the risk is described by probability of a certain event, for example potential loss of life and fatal accident rate [6]. In the nuclear industry the safety is determined by probability of an event due to a particular system. Implementation of passive safety systems allowed to achieve exorbitant standards of core damage frequency of the loss of primary coolant group of 1.37×10^{-7} /year, secondary side breaks of 2.53×10^{-8} /year and steam generator tube rupture of 1.41×10^{-9} /year [1]. All the other systems are characterized with similar frequency.

However, since there is a lack of external driving force, the design of the passive systems requires much more efforts. Furthermore, in order to prove the validity of the design, its operation needs to be verified.

Emergency Condenser (EC) system is one of the concepts for passive heat removal and depressurization of the Reactor Pressure Vessel (RPV) during an accident scenario in the Boiling Water Reactor (BWR). In order to verify the performance, reliability and ability to remove the required amount of heat as well as to draw conclusions regarding the material, wall thickness, and number of tubes of the EC, the operation of a similar system was investigated at a dedicated test facility called NOKO [10]. Based on the outcomes of the test, the Emergency Condenser system in its current form was developed and the system was introduced into KERENA – a new BWR design of Framatome GmbH [12]. Fig. 1 shows a cross section through the reactor [3].

While the tests performed at NOKO were dedicated for optimization of the EC design, in order to examine the performance, reliability and to prove the appropriate safety margins of EC as well as to investigate other passive systems of KERENA in integral tests, a dedicated test facility was built at the Thermal-hydraulics and Components Testing Department of Framatome GmbH in Karlstein, Germany. The Integral Test Facility Karlstein (INKA) represents the KERENA containment with a volume scaling of 1:24. The RPV of KERENA is represented by the steam accumulator of the Karlstein large valve test facility (GAP – Großarmaturen-Prüfstand). The vessel has the storage capacity of 1/6 of the KERENA RPV. In order to simulate the decay heat of the reactor core, the vessel is fed with steam by the Benson boiler with maximum power output of 22 MW [3, 5, 9].

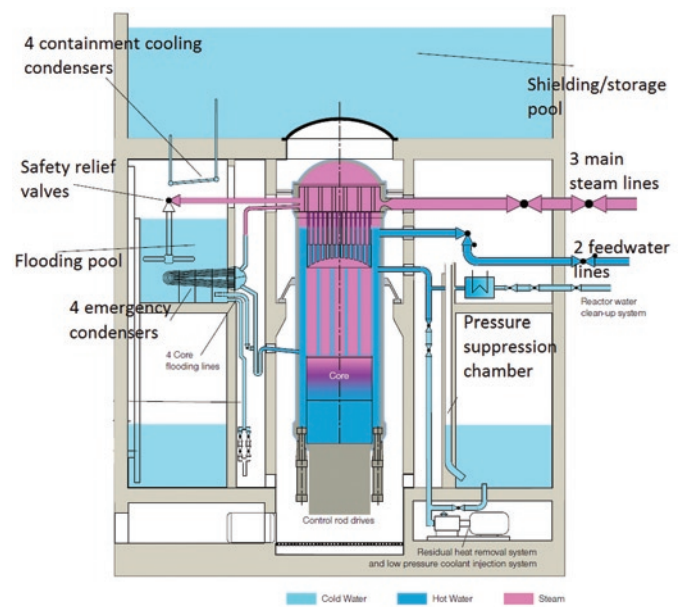


Fig. 1. Cross section through the KERENA containment [3]

One of the purposes of the test facilities of Framatome is to conduct experiments which contribute to validation of codes and models, which may be used in the future to perform pre-calculations before tests, in some cases to eliminate the necessity of conducting test or to help in the design process of new solutions. The current state-of-art codes used for thermal-hydraulic calculations in nuclear industry have been developed for decades. However, they were mainly dedicated for forced flows and their applicability for natural phenomena is still limited. Furthermore, these codes are characterized with low flexibility regarding discretization and they cannot be implemented to several important phenomena, like influence of inert gases on heat transfer. Therefore, efforts have been undertaken to develop a new code for thermal-hydraulics calculation. This code is being developed with a modern and flexible modeling language and it is intended to cover phenomena in passive safety systems of nuclear reactors.

2. Emergency Condenser operation

The main purposes of the Emergency Condenser are to remove heat and to depressurize the RPV in case of an emergency. The system operation principle is illustrated in Fig. 2 [4]. The heat exchange part of the EC is composed of a large number of tubes slightly inclined to horizontal orientation. The pipes are submerged in the cold water which the Flooding Pool Vessel (FPV) is filled with. The EC tubes are also filled with cold water during standard operation of the reactor. In case the liquid water level in the RPV decreases, the water column in the EC-inlet pipe goes down too and the steam from RPV enters the heat exchange piping of the EC system. Since the tube bundle is submerged in the cold water in the FPV, the heat is transferred from the hot medium at the internal side to the cold water in the FPV. EC tubes are slightly inclined, hence the condensate flows back to the RPV due to gravity and the whole EC-RPV system function according to the law of communicating vessels [4].

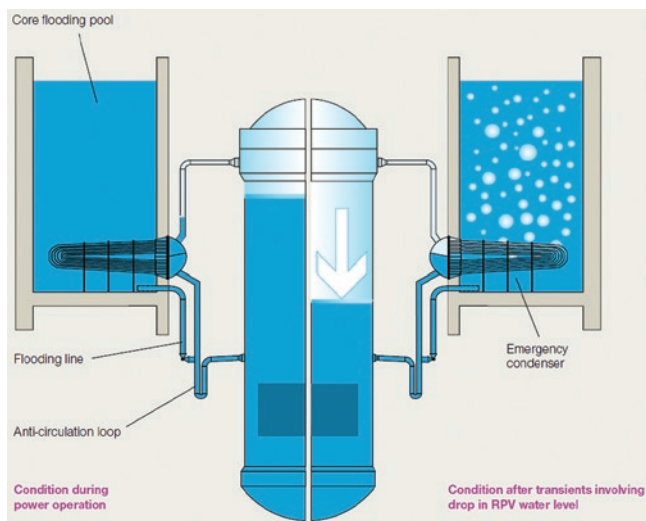


Fig. 2. Emergency Condenser system operation [4]

3. Test setup

INKA test facility may be utilized to perform integral test as well as tests of individual components. Since the purpose of this work was to develop a thermal-hydraulic model which would simulate the behavior of the EC, a test involving only this system was taken as a reference. Fig. 3 shows the setup of the test rig [9].

For the evaluation of the experiments performed at the INKA test facility raw signals are measured and if it is necessary (depending on the parameter of interest) they are processed in order to obtain the values for an assessment.

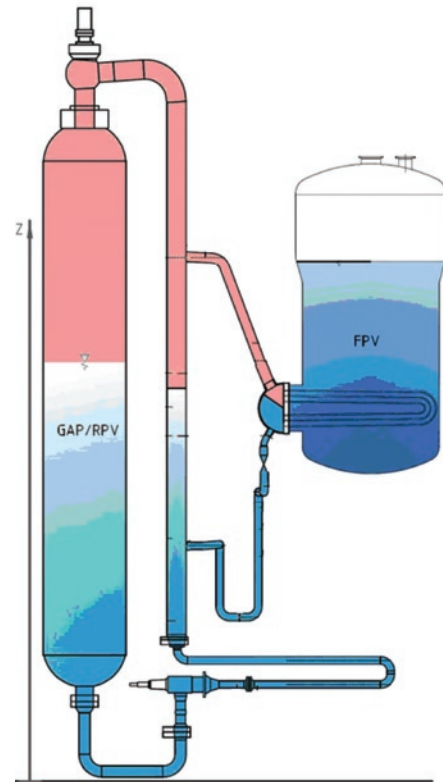


Fig. 3. INKA Test Setup [9]

The processing of data is mostly based on physical principles and mathematical algorithms. For calculation of water properties on the basis of raw signals the formulations given in IAPWS-IF97 is used. In case of more complex calculations e.g. for determination of mass flow several raw signals are utilized together with water tables and the proper formulas in corresponding European norms. A typical uncertainty of temperature measurements is 1.5°C, while the range of pressure sensors uncertainty is between 0.71 and 1.55%, depending on the system. These uncertainties result in the total mass flows uncertainty of 1.03 – 1.9% depending on the system under investigation.

In order to reach the required initial conditions in the system, steam was injected into the RPV/GAP vessel. At the beginning of the test, parameters corresponding to standard BWR operation conditions

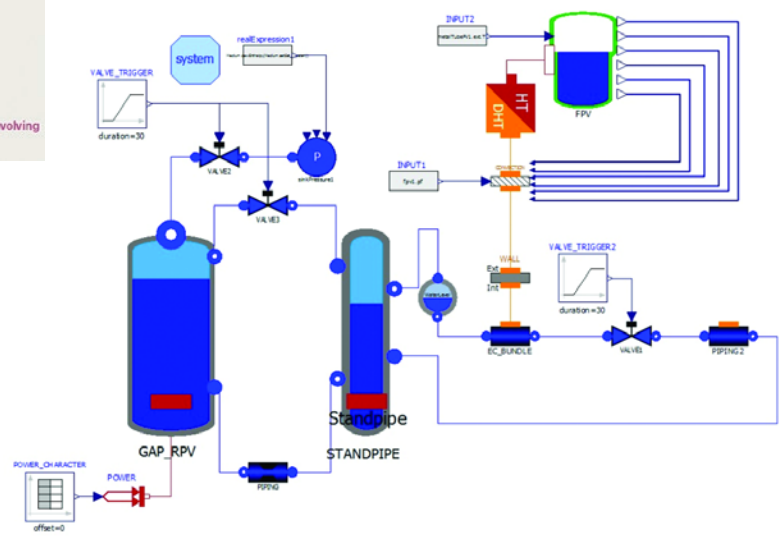


Fig. 4. Diagram view of the model

were set in the vessel. Thus, the temperature was 298°C, pressure was 85 bars and the liquid water level was 11 m. The pressure in the Flooding Pool Vessel was 1 bar and the temperature was 35°C.

The test was initiated by opening the EC return line valve and 15 seconds later the main valve of the RPV, situated at the top of the vessel. Opening of the second valve caused a rapid depressurization of the RPV. This led to the escape of the steam from the RPV, evaporation of the liquid water and to the decrease of the liquid water column height. As expected, this led also to the insertion of the steam from the RPV into the EC tubes and to the heat exchange between the media inside and outside of the EC horizontal tube bundle. The purpose of the test was to evaluate the ability of the EC system to remove the decay heat from the RPV to the FPV.

4. Model development

In order to develop the model, Modelica language and OpenModelica environment was used. Modelica is an object-oriented equation-based modeling language for industrial and academic usage. It is equipped with a large number of libraries dedicated for various domains. In this work Modelica Standard Library and ThermoPower libraries were utilized. In order to model the phenomena of interest, components available in these libraries were developed and extended. A new component representing the FPV was built from scratch. Fig. 4 shows the OpenModelica diagram view of the modeled system.

4.1. Reactor pressure vessel, standpipe, vapor-cold water separator

The RPV and Standpipe are the two large, cylindrical, vertical vessels presented in Fig. 3. The RPV is the one of larger diameter, while the Standpipe is the smaller one. Their Modelica representations are two similar objects on the left side of the Fig. 4. The RPV and Standpipe models are based on dynamic mass and energy balances of liquid and vapor volumes inside the vessels. The mass balance equations are:

$$\frac{dM_l}{dt} = \dot{m}_{cs} - \dot{m}_{evap} + \sum \dot{m}_{port,l} \quad (1)$$

$$\frac{dM_v}{dt} = -\dot{m}_{cs} + \dot{m}_{evap} + \sum \dot{m}_{port,v} \quad (2)$$

where \dot{m} stands for mass flow due to condensation (subscript cs), evaporation (subscript evap) and at the ports (subscript port). M_l and M_v are the total masses of liquid and vapor (subscripts l and v), respectively and they are:

$$M_l = \rho_l V_l \quad (3)$$

$$M_v = \rho_v V_v \quad (4)$$

In (3) and (4) ρ and V represent density and volume. The energy balance equations were introduced for both phases:

$$\frac{dE_l}{dt} = \dot{Q} + \dot{m}_{cs} * h_{ls} - \dot{m}_{evap} * h_{vs} - p \frac{dV_l}{dt} + \sum \dot{m}_{port,l} * h_{port,l} \quad (5)$$

$$\frac{dE_v}{dt} = -\dot{m}_{cs} * h_{ls} + \dot{m}_{evap} * h_{vs} - p \frac{dV_v}{dt} + \sum \dot{m}_{port,v} * h_{port,v} \quad (6)$$

where \dot{Q} represents the decay heat, h specific enthalpy and subscripts vs and ls stand for saturated vapor and saturated liquid, respectively.

The vapor generation due to pressure drop and the decay heat was calculated from the overall energy balance:

$$\frac{d}{dt}(M_l h_l + M_v h_v) = \sum \dot{m}_l h_l + \sum \dot{m}_v h_v + \dot{Q} + \frac{d}{dt}(pV) \quad (7)$$

In the above equation the total change of enthalpy of the vessel is equal to summations of all inputs and outputs of liquid or vapor and the heat delivered through the heat port for simulation of the decay heat of the reactor core. Differentiation of (7) gives:

$$\frac{dM_l}{dt} h_l + \frac{dh_l}{dt} M_l + \frac{dM_v}{dt} h_v + \frac{dh_v}{dt} M_v = \sum \dot{m}_l h_l + \sum \dot{m}_v h_v + \dot{Q} + V \frac{dp}{dt} + p \frac{dV}{dt} \quad (8)$$

Substituting (1) and (2) into (8), neglecting condensation as irrelevant in the analyzed case and taking into account that the volume does not change, the vapor generation due to pressure decrease may be obtained:

$$\dot{m}_{evap} = \frac{-\frac{dh_l}{dt} M_l - \frac{dh_v}{dt} M_v + \dot{Q} + V \frac{dp}{dt}}{h_v - h_l} \quad (9)$$

In order to simulate the decay heat of the reactor core, the heat port was added, so \dot{Q} is added to in the energy balance of liquid water.

The vapor – cold liquid separator situated between the standpipe and the heat exchange section of the EC (Fig. 4) was introduced to separate the phases at the beginning of the test and to enable free flow of vapor once the transient begins and the liquid water level in this component reaches zero as the steam enters the EC heat exchange section.

4.2. Emergency Condenser heat exchange section

The Emergency Condenser heat exchange section consist of a large number of tubes slightly inclined to horizontal orientation. The inclination of the tube is 1.3% and the length of the tube is 10.8 m while their diameter is 48.3 mm. In order to model the flow through the system, an extended version of Flow1DFV2ph component of ThermoPower library was adopted. The flow through the component is governed by mass, energy and momentum conservation equations as one-dimensional, partial differential equations:

$$\dot{m}_{infl} + \dot{m}_{outfl} = \sum_i A l \left(\frac{\partial \rho_i}{\partial h_i} \frac{dh_i}{dt} + \frac{\partial \rho_i}{\partial p} \frac{dp}{dt} \right) \quad (10)$$

$$A l \rho_i \frac{dh_i}{dt} + \dot{m}_i (h_{i+1} - h_i) - A l \frac{dp}{dt} = \dot{Q}_i \quad (11)$$

$$\frac{L}{A} \frac{d\dot{m}}{dt} + p_{outfl} - p_{infl} + \sum_i \Delta p_{g,i} + \sum_i \Delta p_{f,i} = 0 \quad (12)$$

where A represents the pipe cross section and l length of a single volume. Subscripts i , g and f stand for volume number, pressure drop due to gravity and friction, respectively.

The previous study [4] aimed to verify two different approaches to modeling of condensation in horizontal tubes. The first approach was more detailed and it was based on the flow regime map proposed by Tandon [13]. Condensation heat transfer coefficient was calculated for each volume with respect to particular flow regime in this volume. This relatively detailed description of heat transfer in the flow regime based approach was compared against another one, where the heat transfer coefficient was calculated according to one, purely empiri-

cal correlation proposed by Shah [11]. The comparison shown, that both models provide satisfactory results. However, since the single-correlation approach was much simpler, its application led to higher stability of the model and to more time-effective calculations. Therefore, in this work the heat transfer model based on Shah correlation was implemented into the heat transfer module:

$$\alpha = \alpha_{SP} \left[(1-x)^{0.8} + \frac{3.8x^{0.76}(1-x)^{0.04}}{Pr^{0.38}} \right] \quad (13)$$

where x is steam quality, Pr is Prandtl number and α_{SP} is the single-phase heat transfer coefficient calculated by:

$$\alpha_{SP} = 0.023 Re_l^{0.8} Pr_l^{0.4} \frac{\lambda}{D} \quad (14)$$

with liquid Reynolds and Prandtl numbers:

$$Re_l = \frac{\rho_l u D}{\mu_l} \quad (15)$$

$$Pr_l = \frac{\mu_l c_{p,l}}{\lambda_l} \quad (16)$$

where u is the velocity, D is the tube diameter, μ_l is liquid dynamic viscosity, c_p is specific heat capacity and λ_l is the liquid heat conductivity.

The Shah correlation was developed by analysis of a wide spectrum of experimental data, including various fluids and pipe orientations [11].

4.3. Flooding Pool Vessel

Flooding Pool Vessel (FPV) is a water reservoir of large heat capacity. Its aim is to receive the heat from Emergency Condenser piping in case of an emergency and to flood the containment vessel in order to cool the RPV in the event of severe accident.

The Flooding Pool Vessel model was developed from scratch. Since the component does not have any water inputs or outputs, the water mass balance is simply:

$$\rho_l A \frac{dz}{dt} + Az \frac{d\rho_l}{dt} = 0 \quad (17)$$

where z is the water level. The energy balance for the liquid water is given by:

$$\rho_l V_l \frac{dh_l}{dt} - V_l \frac{dp}{dt} - p \frac{dV_l}{dt} = -\dot{Q}_{surface} + \dot{Q}_{EC} \quad (18)$$

In the equation above, \dot{Q}_{EC} is the heat delivered by the EC pipes and $\dot{Q}_{surface}$ is the heat exchange between liquid water and gas and it is calculated as a linear function of temperature difference.

In order to simulate the heat transfer between EC piping and the liquid water inside the FPV, a new heat transfer component was developed. The heat transfer mechanism which is possible at the secondary side is either single-phase free convection or pool boiling. The second one would occur, if the water temperature in the FPV or the heat flux from EC piping was high enough.

Tests performed at INKA indicate that the bubble formation does not take place at the secondary side, so only the first mechanism was taken into account during the development of the heat transfer component. However, indicators informing the user, that the conditions in liquid water in the FPV are close to boiling, were implemented into the model, so that the user knew, that boiling should be considered. Following the VDI Heat Atlas [8], the empirical correlation developed by Bergles [2] was adopted in order to verify, whether the boiling occurs:

$$T_w - T_{sat} = \frac{5}{9} \left[\left(\frac{\dot{q}}{1120} \right)^{0.463} p^{-0.535} \right] p^{0.0234} \quad (19)$$

where T_w and T_{sat} are wall and saturation temperatures, \dot{q} is the heat flux and p is pressure.

The heat transfer at the secondary was calculated according to the correlation for Nusselt number during free convection around a horizontal cylinder [7]:

$$Nu = \left\{ 0.6 + 0.387 * [Ra * f(Pr)]^{\frac{1}{6}} \right\}^2 \quad (20)$$

with Rayleigh and Prandtl numbers calculated according to:

$$Ra = \frac{g l^3 \beta (T_s - T_\infty)}{\nu \kappa} \quad (21)$$

$$Pr = \frac{\nu}{\kappa} \quad (22)$$

where g is the gravity acceleration, β is the water expansion coefficient, ν is the kinematic viscosity and κ is the water thermal diffusivity:

$$\kappa = \frac{\lambda}{\rho c_{p,l}} \quad (22)$$

The function $f(Pr)$ in (20) describes the effect of the Prandtl number over the entire range of Pr and it is given by:

$$f(Pr) = \left[1 + \left(\frac{0.559}{Pr} \right)^{\frac{9}{16}} \right]^{\frac{16}{9}} \quad (23)$$

5. Results and discussion

The test data for the model validation were obtained during an experiment performed at the INKA test facility. The purpose of the test was investigation of the Emergency Condenser system response to sudden decrease of pressure related to loss of coolant accident.

The decrease of pressure was caused by opening of the valve at the top of the GAP vessel during the test. Accordingly, the initiation of the pressure drop was modeled by opening of the valve connecting the RPV with the pressure sink (Fig 4). Fig. 5 presents pressures: measured in the GAP during the test and calculated by the model.

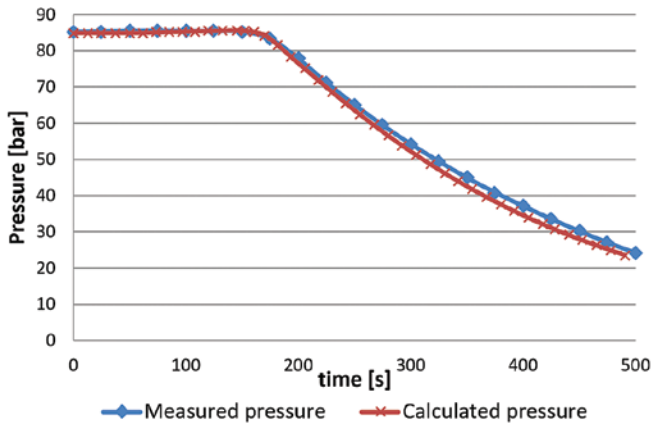


Fig. 5. Pressures—measured during the test and calculated by the model

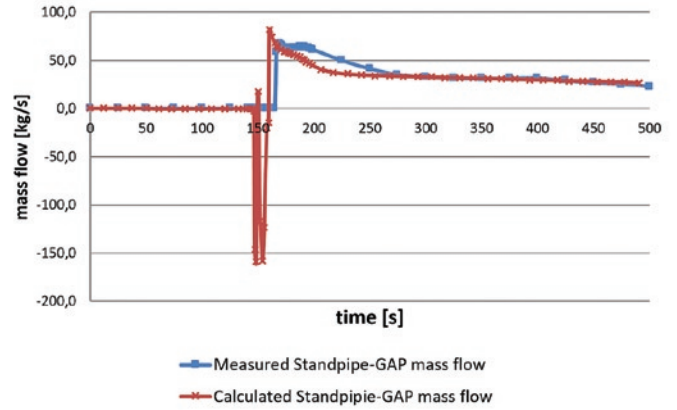


Fig. 6. Standpipe-RPV/GAP mass flows

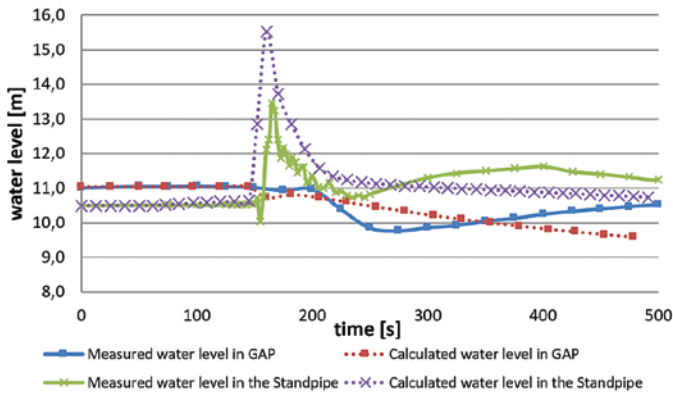


Fig. 7. Water levels – measured during the test and calculated by the model

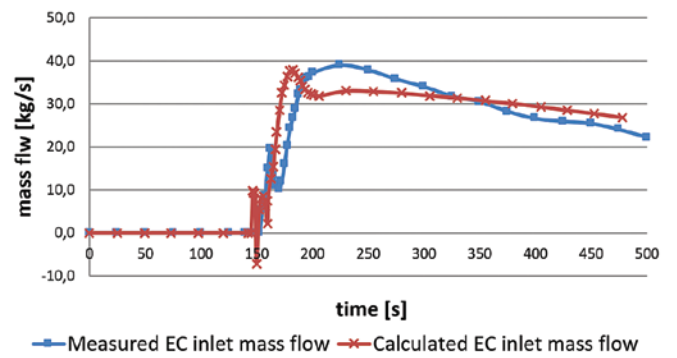


Fig. 8. EC inlet mass flows - measured and calculated

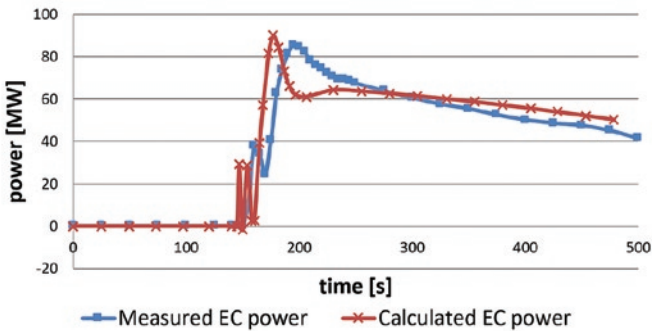


Fig 9. EC power - measured and calculated

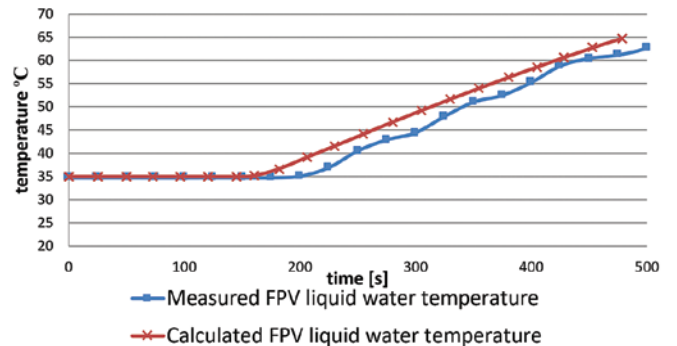


Fig 10. FPV liquid water temperature - measured and calculated

Sudden drop of pressure in the RPV caused strong transients and mass flows between the RPV, Standpipe and the EC heat exchange section. Fig. 6 shows measured and calculated flows between the RPV and the Standpipe.

Fig. 6 shows that according to the model significant peaks of backflow occur at the beginning of the transients. This reverse flow could not be measured due to the instrumentation specification but it partially explains the substantial increase of water level in the Standpipe and the insignificant (due to much larger diameter) decrease in the RPV at the time of the peak. Fig.7 illustrates both water levels.

Apart from the backflow from the RPV, the increase of water level may be explained with opening of the valve separating the EC with the Standpipe. However, even if it was assumed that the EC is totally uncovered i.e. the whole liquid flowed to the Standpipe, the amount of water in the EC tubes would not be enough to cause such a significant increase of water level in the Standpipe. Therefore, both RPV-Stand-

pipe reverse flow as well as flooding the Standpipe by the water in the EC tubes influenced the increase of the water level.

The observed reverse flow is a rather unexpected behavior in the light of the EC operation explained in the section 2. Since the pressure in the RPV decreased, the water started to boil and it is expected that the water column in the Standpipe and EC would cause the flow to the RPV rather than the backflow. However, it should be also considered that once the steam enters the EC piping, it condenses abruptly. This in turn, causes a sudden decrease of pressure in the EC heat exchange section too. Having a very close look at the calculated characteristics of the pressure, mass flows and steam quality at the inlet of EC confirms that a step decrease of the pressure in the steam part of the EC and Standpipe appears exactly at the moment when the steam enters the EC piping. Furthermore, the RPV-Standpipe reverse flow was also observed at exactly the same time. Hence, the obtained simulation results confirm that the significant decrease of pressure due to con-

densation in the EC piping is the reason of initial short-term reverse flow between the RPV and the Standpipe.

Apart from the water levels in the RPV and Standpipe, the described phenomenon should also have an impact on the measured and calculated mass flow at the inlet of the EC heat exchange section. Fig. 8 shows this flow.

Fig. 8 shows that at the beginning of the transients, the effect of the pressure drop due to condensation may be also observed in the mass flow characteristics. Initially the flow is unsteady. Forward and reverse flow may be observed once the EC heat exchange section becomes uncovered and then covered again. As the depressurization in the RPV proceeds, causing evaporation of more and more liquid in this vessel, pressures of the water columns in the Standpipe and EC becomes larger than in the RPV and the flow turns into more stable one.

Insertion of saturated steam into the EC piping and contact of this steam with cold walls forced the heat transfer from the EC to the FPV. Fig. 9 shows measured and calculated values of the EC power.

The measured characteristics was obtained simply by measuring the temperatures at the inlet and outlet of the EC, assuming saturated steam at the inlet, calculating enthalpies and multiplying the enthalpy difference by the mass flow. Similarly to the mass flow characteristics, the calculated power plot shows slightly different behavior in the vicinity of the power peak. In both cases, after initial instabilities, the mass flow and power reach the peak. After this peak a relatively strong decrease of the mass flow and power occurs according to the model. In the test, this drop of around 25% was not observed and the characteristics is a bit milder.

Fig. 9 illustrates that substantial amount of heat is transferred to the FPV. This heat transfer causes obviously an increase of temperature of the liquid in the vessel. Fig. 10 shows the measured water temperature in the FPV together with the one calculated by the model.

Fig. 10 shows that, the measured and calculated temperatures are in a good convergence.

Correspondingly, comparison of all the other characteristics presented in Fig. 5-9 shows that variables are within an acceptable dis-

crepancy and generally that the model correctly represents the system and it may be utilized as a pre-calculation or design-aiding tool. However, it should be also indicated that some time delays between measured and calculated values may be observed. In order to close these gaps, the model should be extended by implementation of additional components so that to represent INKA with more details. However, this may lead to a decrease of the stability and an increase of the calculation time. Hence, the presented degree of detail is a good compromise between calculation time and results quality.

6. Conclusions

In this paper a Modelica representation of the Emergency Condenser system of the INKA test facility was presented and verified against experimental data. The test data cover characteristics of the main parameters of interest during the loss of coolant accident. The purpose of this work was to develop a model, which would correctly evaluate these characteristics.

The EC system is a solution characterized with the highest degree of passivity and the model was developed accordingly. The only parameter impacted both, during the test and in the model was the valve opening to provide the simulated pressure drop. The behavior of the system monitored by other parameters like flows and temperatures was just a spontaneous reaction of the system on the pressure drop.

Presented results show a satisfactory convergence with the test data. In particular the ability to remove the decay heat from the RPV to the FPV was modeled correctly. Since some delays leading to significant discrepancies of the parameters value at a certain moments in time were observed, the model may be improved by insertion of additional components representing the facility in a more detailed way. However, it has to be taken into account, that this actions may decrease the stability of the model and increase the calculation time. Therefore, the presented model may be considered as a reasonable compromise between these aspects and the quality of the results.

References

1. Areva. UK-EPR, Fundamental Safety Overview, Volume 2: Design and Safety, Chapter R: Probabilistic Safety Assessment 2007.
2. Bergles A E. The determination of forced-convection surface boiling heat transfer. *Journal of Heat Transfer* 1964; 86: 365 – 372, <https://doi.org/10.1115/1.3688697>.
3. Bryk R, Schmidt H, Mull T, Ganzmann I, Herbst O. Modeling of the water level swell during depressurization of the reactor pressure vessel of the boiling water reactor in accidental conditions. *Eksplatacja i Niezawodność – Maintenance and Reliability* 2019; 21(1): 28 – 36, <https://doi.org/10.17531/ein.2019.1.4>.
4. Bryk R, Schmidt H, Mull T, Wagner T, Ganzmann I, Herbst O. Modeling of KERENA Emergency Condenser. *Archives of Thermodynamics* 2017; 38(4): 29 – 51, <https://doi.org/10.1515/aoter-2017-0023>.
5. Drescher R, Wagner T, Leyer S. Passive BWR integral LOCA testing at the Karlstein test facility INKA. *VGB PowerTech* 2014; 5: 33 – 37.
6. Flage R, Aven T. Expressing and communicating uncertainty in relation to quantitative risk analysis. *Reliability and Risk Analysis: Theory and Applications* 2009; 2: 9 – 18.
7. Kast W, Klan H, Thess A. Heat Transfer by Free Convection: External Flows. *VDI Heat Atlas: Chapter F2* 2010; 667 – 672, https://doi.org/10.1007/978-3-540-77877-6_120.
8. Kind M, Schröder. Subcooled Boiling. *VDI Heat Atlas: Chapter H3.3* 2010; 804 – 812.
9. Leyer S, Wich M. The Integral Test Facility Karlstein. *Science and Technology of Nuclear Installations* 2012, <https://doi.org/10.1155/2012/439374>.
10. Schaffrath A, Hicken E F, Jaegers H, Prasser H-M. Operation conditions of the emergency condenser of the SWR1000. *Nuclear Engineering and Design* 1999; 188: 303 – 318, [https://doi.org/10.1016/S0029-5493\(99\)00044-8](https://doi.org/10.1016/S0029-5493(99)00044-8).
11. Shah M M. A general correlation for heat transfer during film condensation inside pipes. *International Journal of Heat and Mass Transfer* 1979; 22(4): 547 – 556, [https://doi.org/10.1016/0017-9310\(79\)90058-9](https://doi.org/10.1016/0017-9310(79)90058-9).
12. Stosic Z V, Brettschuh W, Stoll U. Boiling water reactor with innovative safety concept: the generation III+ SWR-1000. *Nuclear Engineering and Design* 2008; 238: 1863 – 1901, <https://doi.org/10.1016/j.nucengdes.2007.12.014>.
13. Tandon T N, Varma H K, Gupta C P. A new flow regimes map for condensation inside horizontal tubes. *Journal of Heat Transfer* 1982; 104(4): 763 – 768, <https://doi.org/10.1115/1.3245197>.

Rafał BRYK

Institute of Heat Engineering, The Faculty of Power and Aeronautical Engineering
Warsaw University of Technology
ul. Nowowiejska 21/25, 00-665 Warsaw, Poland

Holger SCHMIDT

Thomas MULL

Thermal Hydraulics and Components Testing, Framatome GmbH
Paul-Gossen-Straße 100, 91052 Erlangen, Germany

E-mails: rafal.bryk@framatome.com, rafal.bryk@itc.pw.edu.pl,
test-labs@framatome.com
